Received: 14 July 2016 | Accepted: 20 August 2016

DOI: 10.1111/cpr.12295

ORIGINAL ARTICLE

WILEY Cell Proliferation

PCL-PEG-PCL film promotes cartilage regeneration in vivo

Na Fu[1,2#] | Jinfeng Liao[1#] | Shiyu Lin[1] | Ke Sun[1] | Taoran Tian[1] | Bofeng Zhu[3,4] | Yunfeng Lin[1]

[1]State Key Laboratory of Oral Diseases, West China Hospital of Stomatology, Sichuan University, Chengdu, China

[2]School of Stomatology, Hospital of Stomatology, Tianjin Medical University, Tianjin, PR China

[3]Key Laboratory of Shaanxi Province for Craniofacial Precision Medicine Research,College of Stomatology, Xi'an Jiaotong University, Xi'an, Shanxi, China

[4]Clinical Research Center of Shaanxi Province for Dental and Maxillofacial Diseases, College of Stomatology, Xi'an Jiaotong University, Xi'an, Shanxi, China

Correspondence
Prof. Yunfeng Lin, State Key Laboratory of Oral Diseases, West China Hospital of Stomatology, Sichuan University, Chengdu, China.
Email: yunfenglin@scu.edu.cn

Abstract

Objective: Management of chondral defects has long been a challenge due to poor self-healing capacity of articular cartilage. Many approaches, ranging from symptomatic treatment to structural cartilage regeneration, have obtained very limited satisfactory results. Cartilage tissue engineering, which involves optimized combination of novel scaffolds, cell sources and growth factors, has emerged as a promising strategy for cartilage regeneration and repair. In this study, the aim was to investigate the role of poly(ε-caprolactone)-poly(ethylene glycol)-poly(ε-caprolactone) (PCL-PEG-PCL, PCEC) PCEC scaffold in cartilage repair.

Materials and methods: First, PCEC film was fabricated, and its characteristics were tested using SEM and AFM. Cell (rASC – rat adipose-derived stem cells, and mASCs – green fluorescent mouse adipose-derived stem cells) morphologies on PCEC film were observed using SEM and fluorescence microscopy, after cell seeding. Tests of cell viability on PCEC film were conducted using the CCK-8 assay. Furthermore, full cartilage defects in rats were created, and PCEC films were implanted, to evaluate their healing effects, over 8 weeks.

Results: It was found that PCEC film, as a biomaterial implant, possessed good in vitro properties for cell adhesion, migration and proliferation. Importantly, in the in vivo experiment, PCEC film exhibited desirable healing outcomes.

Conclusions: These results demonstrated that PCEC film was a good scaffold for cartilage tissue engineering for improving cell proliferation and adhesion and could lead to excellent repair of cartilage defects.

1 | INTRODUCTION

The repair of articular cartilage defects poses a significant challenge in orthopaedic medicine due to the limited capacity of cartilage to reconstitute its integrated matrix and regenerate native surface. Cartilage is non-vascular, and nutrients are provided by the synovial fluid. On a weight base, it is mainly composed of collagens and proteoglycans. Collagens provide tensile strength, and proteoglycans retain water molecules in the matrix. In humans, cartilage is composed of three zones: superficial, middle and deep zone, each with a distinct composition. The superficial zone includes disc-shaped chondrocytes and the collagen fibres are aligned along the surface. The middle zone has a higher proteoglycan content than the superficial zone; cells are more spherical and the collagen fibres are orientated isotropically. The deep zone contains spherical cells, and collagens have a perpendicular orientation.[1]

Articular cartilage is frequently damaged due to injury or disease. The damaged cartilage cannot fully regenerate because of its limited intrinsic healing capacity. Furthermore, cartilage injuries always lead to secondary degenerative disease of the involved joint such as osteoarthritis (OA).[2,3] OA is the most common form of arthritis, involving cartilage, synovium and bone. The main characteristics are cartilage damage, synovial fibrosis, sclerosis of the subchondral bone and osteophyte formation at the joint margin. To achieve better repair of injured articular cartilage, researchers have optimized clinical methods and proposed various experimental approaches, including abrasion

[#]Na Fu and Jinfeng Liao contributed equally to this work.

arthroplasty,[4,5] microfracture,[5] and transplantation of chondrocytes,[6–9] perichondrium,[10] meniscal allografts,[11] periosteum[12] or osteochondral grafts.[13] In addition, some studies focus on chondrocyte itself. Zhang et al.[14] used the Cre-loxP technique to remove the insulin receptor (IR) from chondrocytes and showed that the loss of IR signalling causes an up-regulation of insulin-like growth factors (IGFs) and insulin-like growth factor (IGF)-1R, which appear to act in a compensatory fashion to regulate the proliferation of chondrocytes. Shen et al.[15] focused on the functional and signalling mechanisms of the TGFb/SMAD pathway, which plays a critical role in articular chondrocytes during OA development. However, to date, there is no satisfactory treatment that enables the full restoration of injured articular cartilage to its original phenotype.

Tissue engineering is a multidisciplinary field, which involves the application of the principles and methods of engineering and life sciences towards the fundamental understanding of structure-function relationships in normal and pathological mammalian tissues and the development of biological substitutes that restore, maintain or improve tissue function. The goal of tissue engineering is to surpass the limitations of conventional treatments based on organ transplantation and biomaterial implantation.[16] It has the potential to produce a supply of immunologically tolerant "artificial" organ and tissue substitutes that can grow with the patient. This should lead to a permanent solution to the damaged organ or tissue without the need for supplementary therapies, thus making it a cost-effective treatment in the long term. Cartilage tissue engineering has emerged as a promising strategy for cartilage repair that holds the key to the successful regeneration of cartilage tissue.[17] Currently, further improvements are needed using desirable scaffold materials with better mechanical and biological functions to be grafted to lesion locations to induce in situ cell differentiation, proliferation and chondrogenesis.

Mesenchymal stem cells (MSCs) are composed of a group of multipotent stem cells derived from adult organs and tissues including bone marrow, ligaments, muscles, adipose tissue and dental pulp.[18–20] MSCs may undergo self-renewal over several generations while maintaining their capacity to differentiate into multi-lineage tissues, such as bone, cartilage, muscle and adipose-derived stem cells (ASCs), as a type of MSC, are readily available. More importantly, ASCs are relatively easy to isolate after removing the excess of adipose tissue by using elective surgery. ASCs supplemented with transforming growth factor beta-1 (TGF-b1) can generate proteoglycan rich spheroids that express collagen II, aggrecan, decorin and other markers consistent with chondrogenesis.[21,22] Subcutaneous implantation in immunodeficient mice showed that ASCs can not only retain the chondrocyte phenotype but can also form cartilaginous tissue.[23]

Poly (e-caprolactone) (PCL) is hydrolytic and cleared by the US Food and Drug Administration for internal use in the human body. A wide variety of tissue engineering applications have demonstrated the ability of PCL to form cell-scaffold complexes in vivo.[24,25] As a typical hydrophilic polymer, PEG is also approved for clinical use by the Food and Drug Administration (FDA). Low molecular weight PEG is readily excreted through kidney.[26] Previous studies have shown that triblock copolymer PCEC has higher degradation rate, hydrophilicity but lower acidity of the derivative products compared with pure PCL, thus exhibiting a good potential in forming cell-scaffold complexes.[27,28] When used as protein and peptide carrier or gene delivery cargo, PCEC microspheres are more ideal than other commonly used PCL and PLA materials, due to the introduction of hydrophilic PEG segments into PCL backbones.[29] Till now, knowledge is still lacking in understanding the role of PCEC scaffold in the repair of cartilage. Therefore, this study is to gain knowledge of the role of PCEC scaffold in the repair of cartilage.

Therefore, in this study, to further mimic the native ECM microenvironment of articular cartilage and improve the biomechanical strength of the scaffold microarchitecture, PCEC film was fabricated and characterized. The cell behaviours of ASCs on PCEC film were examined in vitro. Importantly, we then surgically created full-thickness cartilage defects in rats and implanted PCEC film to evaluate the repair effects within 8 weeks post-surgery. The implantation results based on PCEC film may shed light on its potential in cartilage tissue engineering.

2 | MATERIALS AND METHODS

2.1 | Preparation of PCEC film

The polymer solution was prepared by dissolving 1 g of PCEC (molecular weight: 6.6×10^4, provided by State Key Laboratory of Biotherapy and Cancer Center, Sichuan University, Chengdu, China) in 20 mL of a 4:1 mixture of organic solvent composed of chloroform and dimethylformamide (Sigma, St. Louis, MO, USA). The mixed organic solvent was prepared by rotation (60 rpm) overnight. The PCEC film was obtained by placing the polymer solution in a glass dish (10 cm in diameter and 55 cm^2 in bottom area) and allowing the volatile liquid to evaporate. The thickness of the PCEC film was controlled to be 0.7 mm.

2.2 | SEM

The PCEC film samples were fixed with 5% glutaraldehyde in 1× phosphate-buffered saline (pH=7.4) overnight, dehydrated with increasing concentrations of ethanol (from 30%, 50%, 70%, 90%, 95% to 100%) and lyophilized (FD-1; Bioking Technology Company, Beijing, China). The PCEC film samples were then mounted on aluminium stumps, coated with gold in a sputtering device for 1.5 min at 15 mA and examined under a scanning electron microscope (SEM; HITACHI S-4800, Tokyo, Japan) equipped with an EDS (Alpha Ray Spectrometer, Oxford, UK) at an accelerating voltage of 20 kV. The diameter of the PCEC film was measured from the SEM images using image analysis software (Image J, National Institutes of Health, Maryland, USA) and calculated by randomly selecting 100–150 fibres in the SEM images.

2.3 | AFM

The surface roughness of the PCEC film was measured using an atomic force microscope (AFM, Nanoscope MultiMode & Explore SPM, Vecco Instrument, New York, US) operated in ambient air under tapping mode with a scan rate of 0.5 Hz and a scan size of 5 × 5 μm^2. The root mean square (RMS), surface area difference, and Z range were estimated with the aid of Nanoscope imaging software.

2.4 | Contact angle measurement

For the determination of hydrophilicity of the scaffolds, the static contact angle of distilled water on the surface of the PCEC film was measured using a Cam 200 optical contact angle meter (KSV Instruments, Monroe, CT, USA). The images of water drops on the sample surface were obtained using a CCD camera (KGV-5000, Japan) and then analysed with software supplied by the manufacturer. Six samples were measured in each group. Four different points were measured for each sample. Initially, distilled water (5 mL) was used in each measurement after exposure for 3 seconds at ambient temperature and 65% relative humidity (RH).

2.5 | Mechanical testing parameters

The mechanical properties of the PCEC film were determined using a tabletop uniaxial testing instrument (Instron 5565, Minnesota, USA) equipped with a 50 N load cell under a crosshead speed of 5 mm min^{-1} under ambient conditions (RH ~65%). All the samples were prepared in rectangular shape with dimensions of 10 × 60 mm^2 from the PCEC film. The mechanical testing was repeated at least six times. The stress–strain curves, Young's modulus and elongation at break of the PCEC film were obtained.

2.6 | Cell culture

Animal materials used for this study were obtained according to governing ethical principles, and our protocol was reviewed and approved by our institutional review board (IRB).

rASCs were isolated from subcutaneous adipose tissue from groins of 2-week-old SD rats, which were from the Sichuan University Animal Center. Collected tissues were cut into small pieces and digested in 0.075% type-I collagenase (Sigma-Aldrich) solution in a shaking incubator for 60 minutes. This was then neutralized 1:1 (v/v) with 10% heat-activated foetal bovine serum (FBS) a-MEM (0.1 mmol L^{-1} non-essential amino acids, 4 mmol L^{-1} L-glutamine, 1% penicillin–streptomycin solution), and suspensions were centrifuged at 157 ×g for 5 minutes. After removal of supernatants, remaining rASCs were resuspended in 10% FBS a-MEM and seeded into plates or T25 flasks, then incubated at 37°C in a 5% CO_2 incubator. Cells were subcultured to passage three for further experimentation.

To obtain green fluorescent protein-positive ASCs, subcutaneous adipose tissue was collected from enhanced green fluorescent protein (GFP) transgenic mice (Centre for Genetically Engineered Mice, West China Hospital, Sichuan University, Chengdu, China). The green fluorescent protein-positive ASCs was obtained under sterile conditions from GFP transgenic mice as the method described above for rASCs.

2.7 | Cell morphology

The PCEC films (which were cut into a round shape fitting the well diameter in a 96-well plate with a thickness of 0.7 mm) were placed into 96-well plates. All the materials were irradiated under ultraviolet light for half an hour for disinfection.

The third passage of green fluorescent protein-positive mASCs was seeded at 5–10 × 10^4 per mL density into the glass-bottomed 96-well plates, which were prepared as described above. For comparison purposes, the control group, in which the green fluorescent protein-positive mASCs were seeded at the density of 5–10 × 10^4 per mL into the six-well plates without the scaffold materials, was established. For each group, two parallel holes were set up. The cells were studied using an Olympus IX 710 microscope (Olympus, Tokyo, Japan) after cultured in the basic medium for 1, 5 and 5 days.

For SEM, the third passage of rASCs was seeded at 5–10 × 10^4 per mL density into the glass-bottomed 96-well plates, which were prepared as described above. After cells seeding for 1, 3 and 5 days, the cells that were attached and infiltrated into the PCEC film were fixed with 3% glutaraldehyde for 1 hour, rinsed three times in water and dehydrated with graded concentrations of ethanol (percentage from 50, 70, 90 to 100, v/v). Subsequently, the samples were treated with hexamethyldisiloxane (HMDS) and kept in a fume hood for air drying. Finally, the samples were coated with gold for the observation of their cell morphologies.

2.8 | Cell proliferation assay

For cell proliferation, the cell counting assay kit-8 (CCK-8) (Dojindo, Kumamoto, Japan) was used to quantify the amount of viable cells to determine the extent of cell proliferation and cytotoxicity on the PCEC film after the third passage of rASC seeding at the density of 10^5 per mL for 1, 3 and 5 days. Briefly, 10 mL of CCK-8 solution was added to each well of a 96-well plate with or without the scaffolds. The loaded samples were incubated at 37°C for 1–4 hours to form water insoluble formazan. The optical density (OD) value was measured at a wavelength of 450 nm using a microplate reader (VariOskan Flash 3001; Thermo, New York, USA). The amount of the formazan dye generated by the activity of dehydrogenases in the cells was directly proportional to the number of living cells. The samples included the normal control group and PCEC film groups; all the treated groups were normalized to the control group.

2.9 | In vivo cartilage defect formation

Animal materials used for this study were obtained according to governing ethical principles, and our protocol was reviewed and approved by our institutional review board (IRB).

Thirty 12-week-old SD rats from the Sichuan University Animal Center were used in this study. The animals were anaesthetized with chloral hydrate by intraperitoneal injection. A medial parapatellar skin incision was made, and the knee joint was exposed *via* lateral dislocation of the patella. Full-thickness cartilage defects that extend through the cartilage layer and penetrate the subchondral bone were created surgically at the femoropatellar groove of both the hind leg knee joints. The defects were made with a diameter of 1.5 mm and a depth of 2 mm as previously described.

2.10 | In vivo implantation

PCEC films (which were cut into a round shape with a diameter of 1.5 mm and a thickness of 0.7 mm) were placed into 96-well plates

for half an hour under ultraviolet disinfection. Twelve-week-old[30] SD rats were used to generate 60 defect samples (bare PCEC scaffolds: 40 samples and chondrocyte defects without treatment: 20 samples [controls]). Immediately after the formation of the cartilage defect in rats, the implantation was carried out by filling the overlapped scaffolds into the defect holes. Rats were killed after 4 (10 rats, 20 samples) and 8 (10 rats, 20 samples) weeks to assess the repair process of cartilage effects. The defects were made with a diameter of 1.5 mm and a depth of 2 mm; thus, we used the film with a diameter of 1.5 mm and thickness of 0.7 mm to fill the defects. The specific methods used are as follows: we first placed a layer of PCEC film on the defect through extrusion to stabilize the PCEC film in the defect region until the defect area was filled.

2.11 | Histological staining and immunohistochemistry

For histological evaluation, the implantation sites were harvested and fixed in 4% PFA for 48 hours at 4°C. Samples were treated with a series of graded alcohol baths for dehydration, and then they were treated with xylene, embedded in paraffin and sectioned into slices with a thickness of 5 mm. The sections were stained with haematoxylin and eosin (HE, Beyotime, China), Safranin O (Sigma-Aldrich).

For immunohistochemistry, the slices were stained with rat polyclonal antibodies against rat type-II collagen (no. bs-0709R; Bioss, Beijing, China) and goat anti-rat IgG/biotin (no. SP-0023; Bioss) according to a standard SABC protocol reported by the manufacturer. The rehydrated paraffin sections were treated with 0.1% trypsin for epitope unmasking before staining. Three samples for each group were analysed using an inverted light microscopy (Olympus-IX71).

2.12 | Statistical analysis

The results are expressed as mean ± standard deviation. Statistical analysis was performed using the Student's *t* test and one-way analysis of variance (ANOVA) followed by analysis using SPSS 19.0 software (SPSS, Chicago, IL, USA). In each analysis, the critical significance level was set at $P<.05$.

3 | RESULTS

3.1 | Characteristics of PCEC film

The morphologies of PCEC film were first characterized by SEM (Fig. 1a) and AFM (Fig. 1b). The SEM results show that the topological

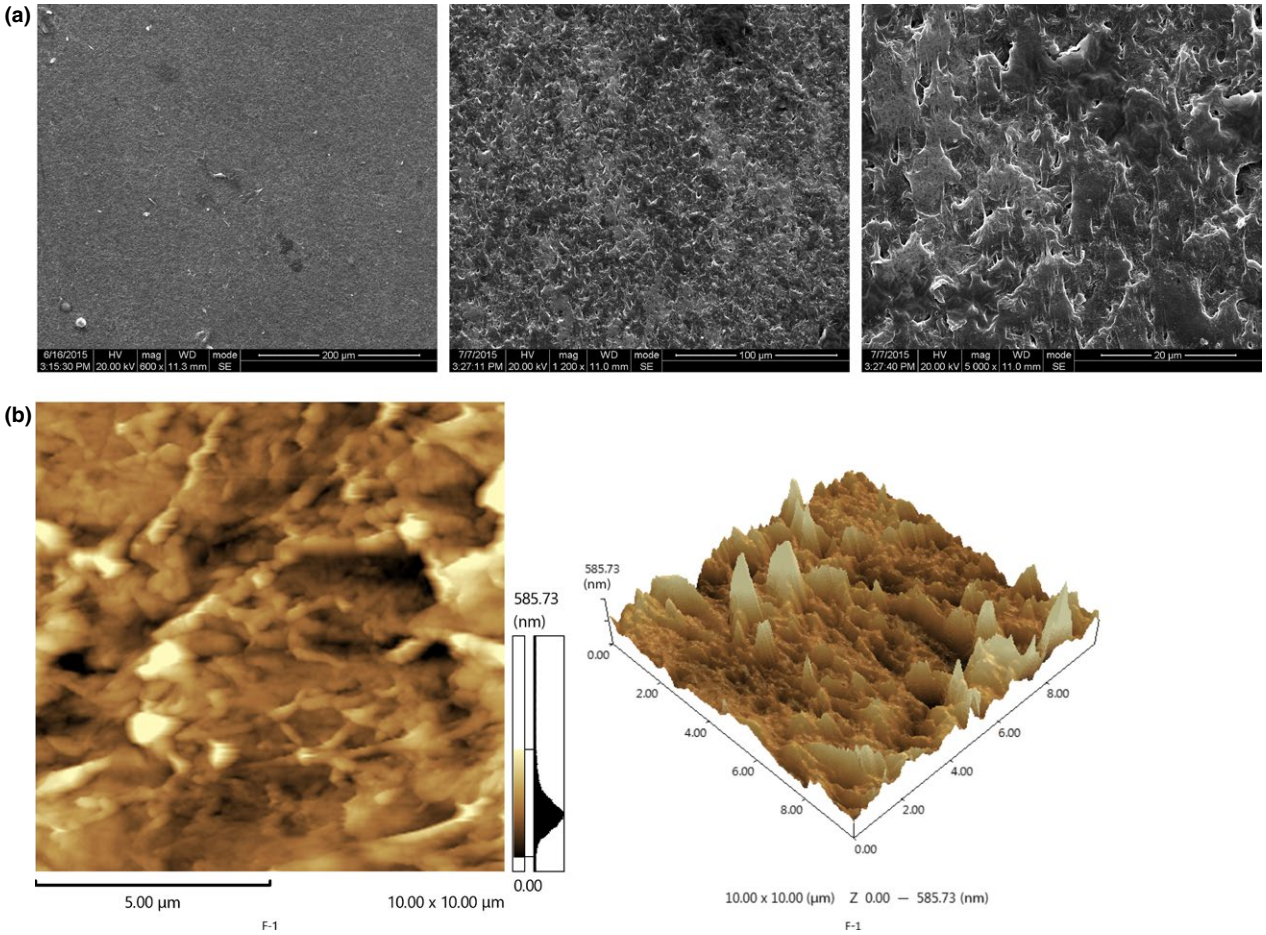

FIGURE 1 The morphologies of PCEC film. (a) Morphology of the PCEC film evaluated by SEM (n=3). The topological structure of the PCEC film had no fibres, and the surface was relatively smooth and featureless. (b) Morphology of the PCEC film evaluated by AFM (n=3). The topological structure of the PCEC film was detected randomly at 10 × 10 µm. The quantified surface roughness was 585.73 nm in height

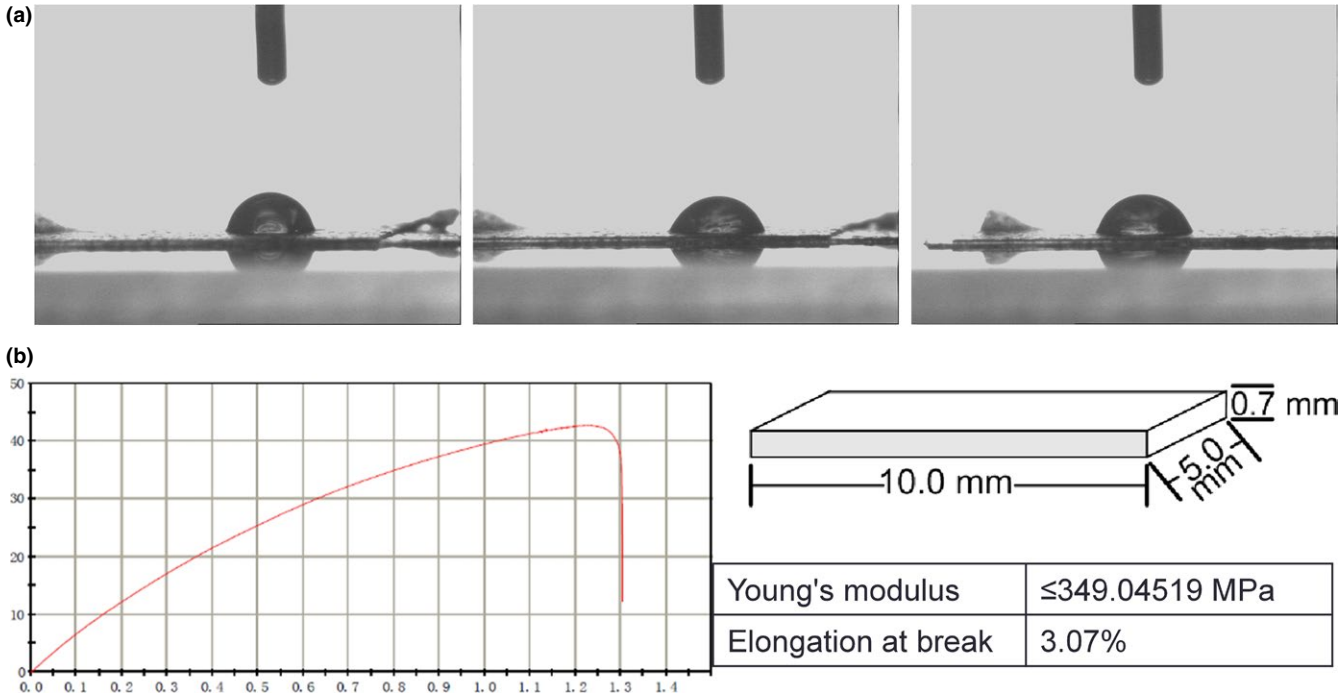

FIGURE 2 Characterization of PCEC film. (a) Measurement of the water contact angle wetting behaviour of a water droplet on the PCEC film (n=3), the contact angle was determined at 69.23 ± 1.5°. (b) Mechanical parameters determined from slices of the PCEC film (10.0 × 5.0 × 0.7 m^3) (n=3). The PCEC film could bear the tensile force up to 6 N, and the tensile displacement reached ~3 mm before its fragmentation and the Young's modulus was approximately 349.04519 MPa and the elongation at break was 3.07%

structure of the PCEC film had no fibres and the surface was relatively smooth and featureless. For AFM, to show a representative topological morphology, we chose a random size of 10 × 10 μm. The quantified surface roughness was about 585.73 nm in height. Because the PCEC film featured a high specific surface area, one of the decisive factors for micro-scale materials was wettability; the contact angle was determined to be 69.23 ± 1.5° by a Cam 200 optical contact angle meter instrument (Fig. 2a). In the tension test (Fig. 2b), the PCEC film could bear the tensile force up to 6 N, and the tensile displacement reached ~3 mm before its fragmentation. At the scaffold size of 10 × 5 × 0.7 mm^3, mechanical parameters were measured. Young's modulus was about 349.04519 MPa and the elongation at break was 3.07%.

3.2 | Cell behaviours of ASCs in response to the PCEC film in vitro

The ASCs from green fluorescent mice were seeded onto the PCEC film and the green fluorescent protein-positive mASCs attached to the PCEC film after seeding (Fig. 3). In the Petri dish containing the control group, green fluorescent protein-positive mASCs were seeded, attached, spread and proliferated within 5 days. For the PCEC film as well, at day 3 after seeding, the cell spreading area was the broadest. Then, the number of green fluorescent protein-positive mASCs was significantly increased and was up to confluence at day 5. And the numbers increased as compared with the control group. The SEM images of the attached rASCs are shown in Fig. 4a. At day 3 after seeding, the cell spreading area was the broadest. Then, the number of rASCs was significantly increased and was up to confluence at day 5. The proliferation assay was performed to evaluate the cell proliferation rate on the scaffolds using the CCK-8 assay kit (Fig. 4b). The results showed that after day 1, 3 and 5, the rASCs on the PCEC film had a significantly higher proliferation rate than those found on the Petri dish group.

3.3 | Knee cartilage defect and biomaterial implantation: PCEC film in cartilage tissue engineering

PCEC film could fill the site of cartilage defect due to its good mechanical properties and biocompatibility. During the in vivo experiments, full-thickness cartilage defects were created on the hind knees of 12-week-old SD rats. The sites of the defects were surgically created at the femoropatellar groove (1.5 mm in diameter, 2 mm in depth). The groups were divided into two subgroups including the PCEC film implant group (20 rats, 40 samples) and bare chondrocyte defect group without any treatment (10 rats, 20 samples). The wounds were sutured immediately after the scaffold materials were implanted. Animals post surgery maintained good health throughout the study, as assessed by their weight gain. The experimental rats were killed and the repair of the cartilage defects was detected at 4 and 8 weeks post-surgery. At week 4, the new-formed tissues could not cover the defects in all groups. At week 4, the implantation group showed integral repair morphology, but the interface between the scaffolds and newly formed tissue was clearly visible. At week 8, the implantation

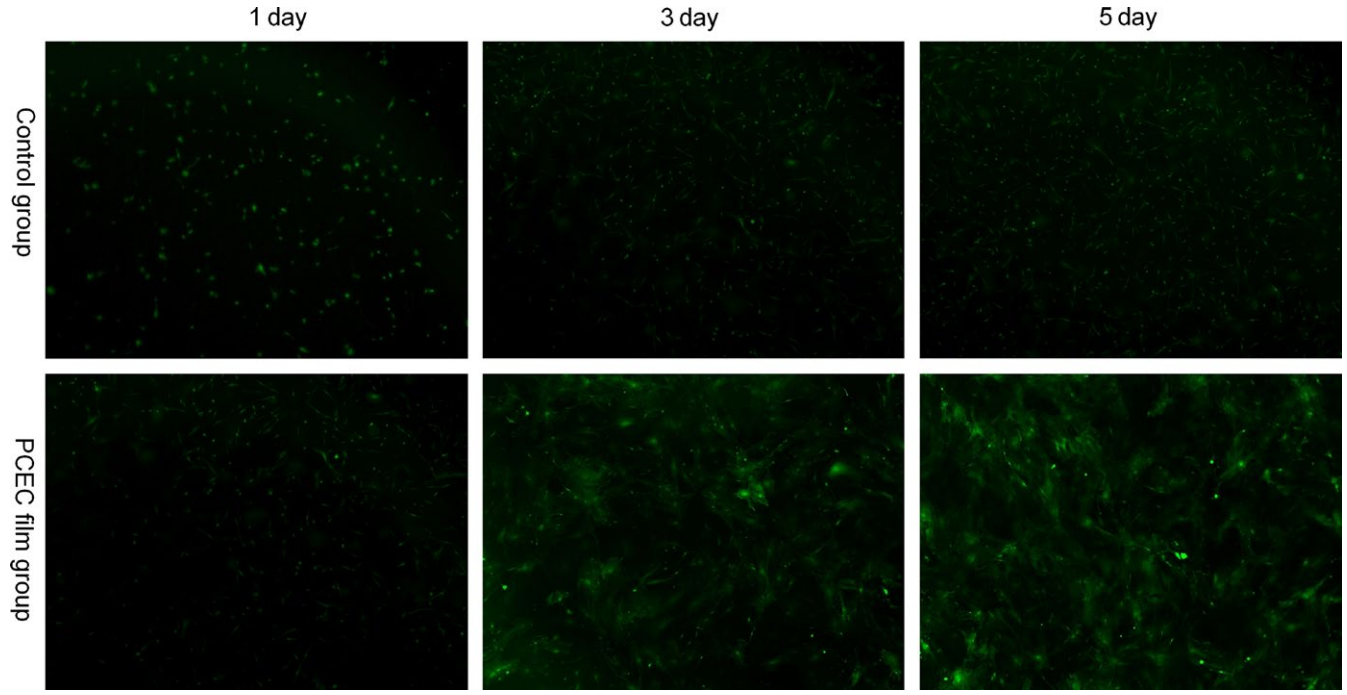

FIGURE 3 Architectural characteristics of the PCEC film elucidated by the morphology of ASCs from green fluorescent mice, as shown by microscope observation, green fluorescent protein-positive mASCs were seeded on the PCEC film at different days. The Petri dish group showed the normal morphologies of cultured green fluorescent protein-positive mASCs at different days (n=3). By 5 d after seeding, the cells attached to the PCEC film, significantly increased in numbers, in comparison to the other group

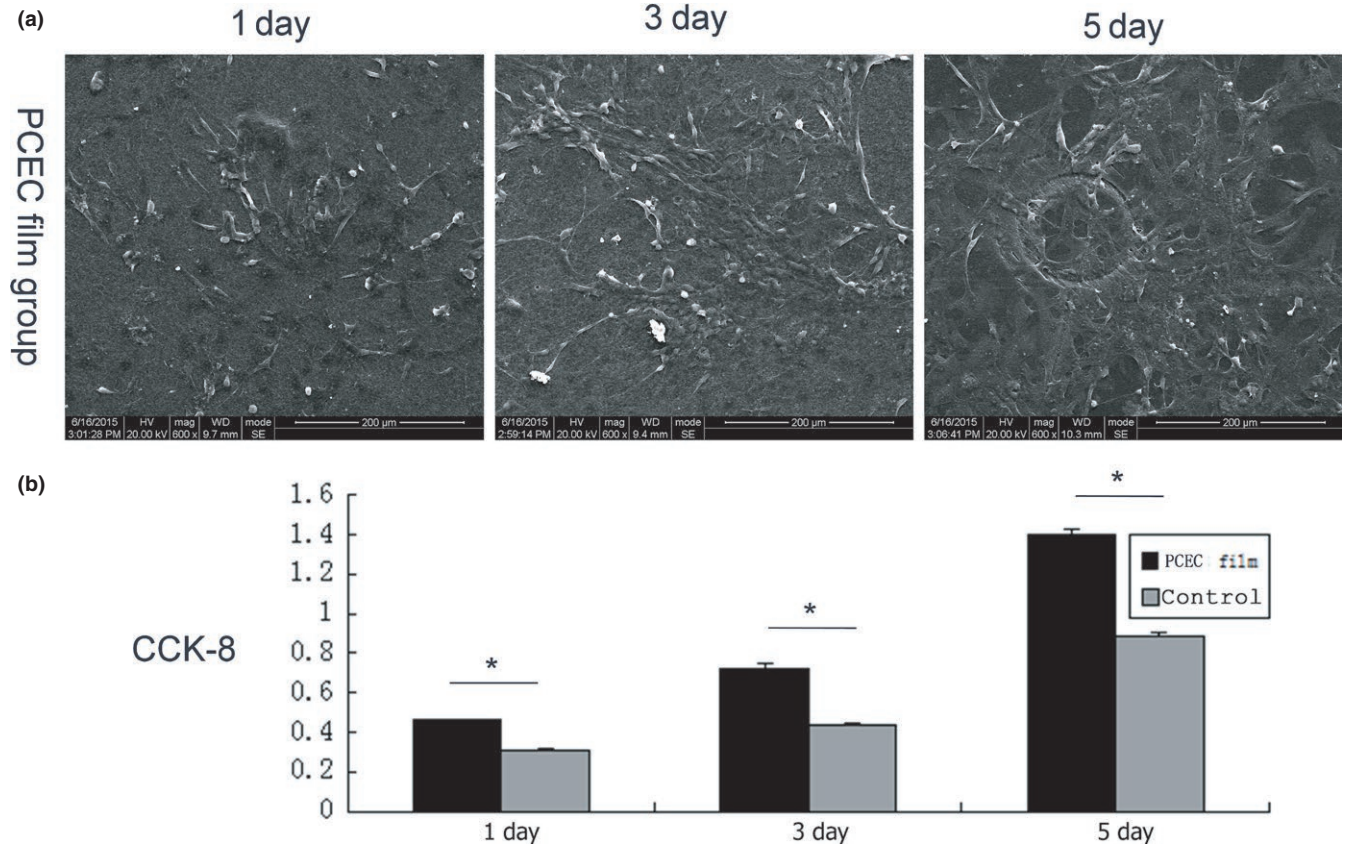

FIGURE 4 In vitro cell behaviour of the PCEC film. (a) Cell morphologies of mASCs on the PCEC film for implantation, as shown by SEM (n=3). mASCs were seeded, attached, spread and proliferated within 5 d. (b) Cell proliferation of mACSs on the PCEC film and Petri dishes (n=3). The results show that the proliferation rates within 5 d were significantly higher on the PCEC films than that found on the Petri dishes

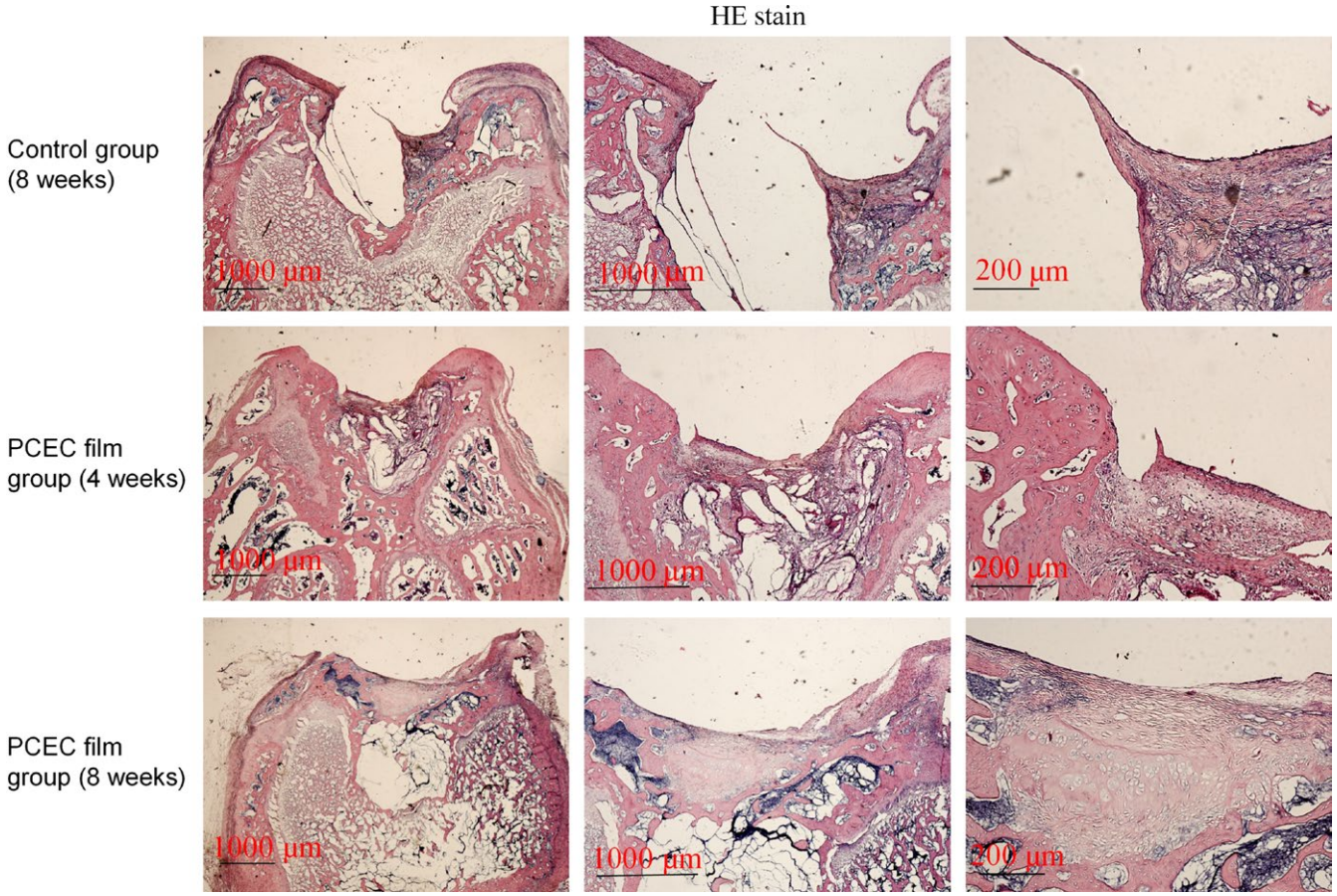

FIGURE 5 HE staining of cross-sections of repaired knee articular cartilage at 4 and 8 wk. HE staining showed the interfaces between the peri-native tissues and new-formed tissues in all the groups. The control group (8 wks) showed a reduced defect area but did not form repair morphology. Among the implant groups, the interfaces were more distinct at 4 wks than at 8 wks post-surgery. At 8 wks, repaired newly formed tissue gradually covered the implanted films to form an integral cartilage-like tissue. The experiments were repeated three times (n=3)

groups had formed repaired morphologies for the cartilage defect, and the newly formed tissue covered the whole defect zone and the interface between the scaffolds and the newly formed tissue disappeared. The control group (8 weeks) showed a reduced defect area but did not form repair morphology like native cartilage. The defect area is covered by the new tissue, but most of the new tissue was connective tissue which was relatively loose, and the PCEC film implant indentation of cartilage defects showed integral repair morphology but the embedded PCEC film did not show any degradation.

3.4 | Repair evaluation: from histological staining to immunohistochemistry

The samples from the repair sites of the cartilage defects at 4 and 8 weeks post-surgery were evaluated by HE, Safranin O, type-II collagen staining (Figs 5–7). HE staining showed the interfaces between the peri-native tissues and new-formed tissues in all the groups. The control group (8 weeks) showed a reduced defect area but did not form repair morphology. Among the implant groups, the interfaces at 4 weeks were more distinct when compared with those at 8 weeks post-surgery. At 4 weeks, the layers of the PCEC film were clearly shown, but the newly formed tissue (Fig. 5) was gradually covered at the top of cartilage defect indentation. At 4 weeks, the original tissue, newly formed tissue and PCEC film were all clearly observed at the site of the cartilage defect. At 8 weeks, an improved repaired new-formed tissue gradually covered the PCEC film to form integral cartilage-like tissue. One of the most important markers for evaluating cartilage repair is the assembly of proteoglycan. The internal repair integrity was shown in scaffold-implanted groups by Safranin O staining and was especially clear in the implant group, and we found that the control group (8 weeks) showed a reduced defect area but did not form repair morphology. Among the implant groups, at 4 weeks post-surgery, there were distinct differences between the original tissue and newly formed tissue. The newly formed tissue showed a light colour relative to the original tissue, although the newly formed tissue showed the component of proteoglycan. At 8 weeks, the newly formed tissue completely covered the implant material and formed an integral surface with a thickness of ~400 mm. However, the PCEC films were embedded in the deep defects and did not degrade (Fig. 6). We further evaluated the components of proteoglycan and collagen II at the repair sites using type-II collagen staining (Fig. 7). Type-II collage is another important marker used to evaluate the cartilage repair. The

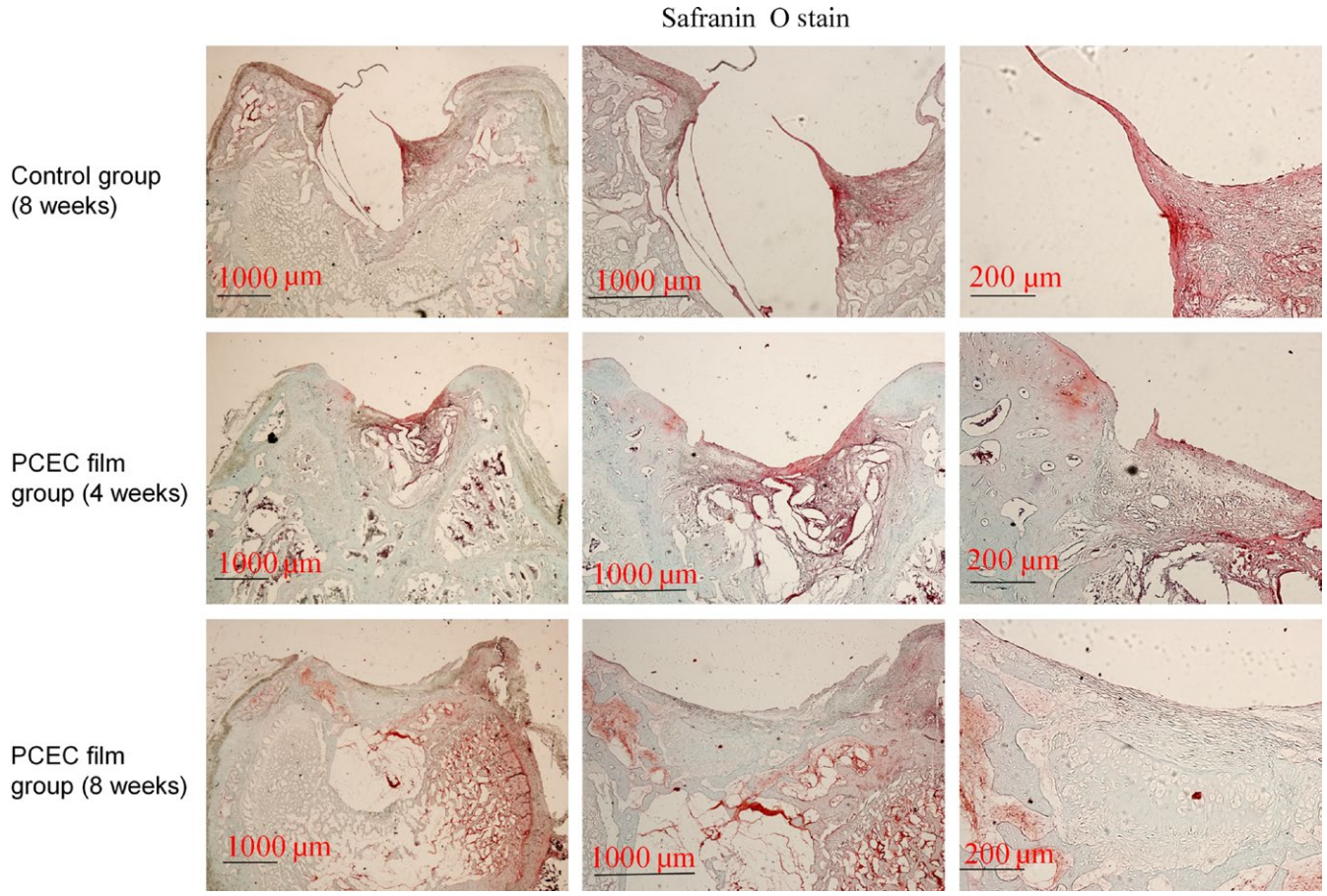

FIGURE 6 Safranin O staining of cross-sections of repaired knee articular cartilage at 4 and 8 wk. One of the most important markers for evaluating cartilage repair is the assembly of proteoglycan. The internal repair integrity was shown in scaffold-implanted groups by Safranin O staining and was especially clear in the implant group. We found that the control group (8 wk) showed a reduced defect area but did not form repair morphology. Among the implant groups, at 4 wk post-surgery, the newly formed tissue showed a light colour relative to the original tissue, although the newly formed tissue showed the component of proteoglycan. At 8 wk, the newly formed tissue completely covered the implant material and formed an integral surface with a thickness of ~400 mm. However, the PCEC films were embedded in the deep defects and did not degrade. The experiments were repeated three times (n=3)

interfaces between peri-native and newly formed tissue were distinct among control and implant group. We found that the control group (8 weeks) showed a reduced defect area but did not form repair morphology. Among the implant groups, the interfaces between the peri-native tissue and new-formed tissue were distinct at 4 weeks. At the top of the indentation of the cartilage defects, a thin layer of type-II collagen containing new tissue was formed and this newly formed tissue did not form an integral surface. At 8 weeks, the original tissue and newly formed tissue were fused and an integral surface was formed.

4 | DISCUSSION

The goal of tissue engineering is to furnish living structures that have the potential to integrate with surrounding tissue. Central to formation of newly regenerating tissue is the scaffold which is providing its support. The role of the scaffold is to provide anchorage for cells while permitting sufficient bone blood flow. Prior investigations have demonstrated the ability of mineralized bone to form in vitro on porous biodegradable polymer scaffolds. A wide variety of scaffold fabrication techniques has been developed, for example, solvent casting/porogen leaching,[30,31] phase separation,[32,33] emulsion freeze drying,[34] gas foaming[35] and electrostatic spinning.[36,37] For treatment of large bone defects, scaffolds should enable blood vessel ingrowth by providing the appropriate architecture and signalling for angiogenesis.

Biomimetic scaffolds using natural and synthetic biomaterials are highly desirable to recreate the micro-architecture of articular cartilage. Some studies have suggested that environmental,[38] cytokines and suitable scaffold materials can promote bone and cartilage tissue regeneration.[39–45] Although intensive research has focused on the developmental biology and regeneration of cartilage tissue, and a diverse plethora of biomaterials have been developed for this purpose, cartilage regeneration is still suboptimal with disadvantages, such as lack of a layered structure, mechanical mismatch with native cartilage, and inadequate integration between native tissue and the implanted scaffold.[46,47]

Adipose-derived stem cells are emerging as a promising option for treating tissue damage and diseases because of their accessibility and

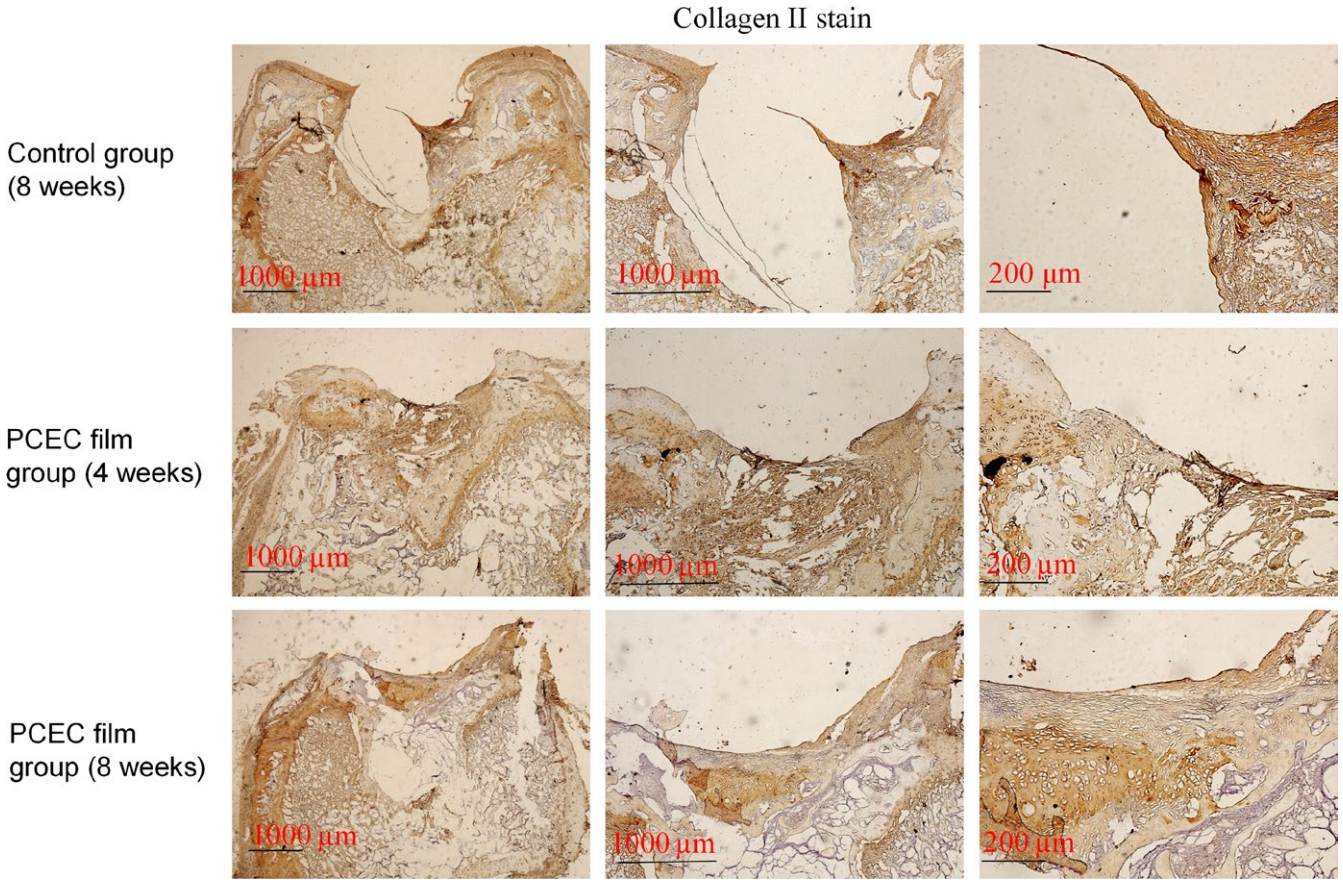

FIGURE 7 Type-II collagen staining of cross-sections of repaired knee articular cartilage at 4 and 8 wk. Type-II collage is another important marker used to evaluate the cartilage repair. The interfaces between peri-native and newly formed tissue were distinct among control and implant group. We found that the control group (8 wk) showed a reduced defectarea but did not form repair morphology. Among the implant groups, the interfaces between the peri-native tissue and newly formed tissue were distinct at 4 wk. At the top of the indentation of the cartilage defects, a thin layer of type-II collagen containing new tissue was formed and this newly formed tissue did not form an integral surface. At 8 wk, the original tissue and newly formed tissue were fused and an integral surface was formed. The experiments were repeated three times (n=3)

their ability to differentiate into multiple cell lineages, including chondrocytes. ASCs have also been used to enhance muscle regeneration, promote neovascularization and reossify large cranial defects. ASCs can also undergo chondrogenic differentiation.

Zhang et al.[48] have reported that PCEC exhibited good potential in forming cell-scaffold complexes because of its high biodegradation rate, amphiphilic nature and biocompatibility. In our study, the characteristics of PCEC film were tested using SEM and AFM. Cell morphologies on PCEC film were obtained using SEM and fluorescence microscopy after cell seeding. The tests of proliferation on PCEC film were conducted using CCK-8 assay. It was found that PCEC film, as a biomaterial implant, possessed good in vitro properties for cell adhesion, migration and proliferation. After characterizing the PCEC film, we found it as a relatively favourable natural biomaterial that is suitable for implantation in cartilage defects, especially because of its intrinsic hydrophilicity. So next full cartilage defects in rats were created and PCEC films were implanted to evaluate their healing effects within 8 weeks. The results show that in the in vivo experiment, PCEC film exhibited desirable healing outcomes.

There are still some limitations in this study. First, the investigation that whether the newly repaired tissue is a cartilaginous tissue or fibro-cartilaginous tissue needs a long-term follow-up, although the morphology, histological staining and immunohistochemistry have confirmed the markers of cartilage in the new-formed tissues. And in the control group, the defect area is covered by the new tissue, but most of the new tissue was connective tissue which was relatively loose, so the connective tissue is easy to fall off in the process of slicing and dyeing. Second, the time during which PCEC film could entirely degrade and the new cartilage could be completely formed should be confirmed. Third, whether the mechanical properties of the newly formed tissues are closed to those of native cartilage also needs to be further investigated.

5 | CONCLUSIONS

In this study, the PCEC film was fabricated and its mechanical properties were determined. Adipose-derived stem cells (ASCs) were seeded

onto the film to evaluate their abilities of adhesion and proliferation. It was established that the cells seeded onto the films had better abilities of adhesion and proliferation in vitro. Furthermore, the actual thickness cartilage defects were created at the site of the femoropatellar groove of rat knees and the PCEC film scaffold was immediately implanted. Eight weeks post surgery, new cartilage-like tissues were formed at the sites of the defects. Evaluation from histological staining to immunohistochemistry confirmed a better integration between the native tissues and scaffolds. Our findings demonstrate that the PCEC film scaffold shows great potential in the field of tissue engineering and could lead to excellent repair of cartilage defects.

ACKNOWLEDGEMENTS

This work was funded by the National Natural Science Foundation of China (81470721), Sichuan Science and Technology Innovation Team (2014TD0001).

REFERENCES

1. Kuettner KE, Cole AA. Cartilage degeneration in different human joints. *Osteoarthritis Cartilage*. 2005;13:93–103.
2. Jackson DW, Simon TM. Chondrocyte transplantation. *Arthroscopy*. 1996;12:732–738.
3. Newman AP. Articular cartilage repair. *Am J Sports Med*. 1998;26:309–324.
4. Bert JM. Role of abrasion arthroplasty and debridement in the management of osteoarthritis of the knee. *Rheum Dis Clin North Am*. 1993;19:725–739.
5. Johnson LL. Arthroscopic abrasion arthroplasty historical and pathologic perspective: present status. *Arthroscopy*. 1986;2:54–69.
6. Brittberg M, Lindahl A, Nilsson A, Ohlsson C, Isaksson O, Peterson L. Treatment of deep cartilage defects in the knee with autologous chondrocyte transplantation. *N Engl J Med* 1994;33:889–895.
7. Grande DA, Pitma MI, Peterson L, Menche D, Klein M. The repair of experimentally produced defects in rabbit articular cartilage by autologous chondrocyte transplantation. *J Orthop Res*. 1989;7:208–218.
8. Katsube K, Ochi M, Uchio Y, et al. Repair of articular cartilage defects with cultured chondrocytes in Atelocollagen gel. Comparison with cultured chondrocytes in suspension. *Arch Orthop Trauma Surg*. 2000;120:121–127.
9. Shortkroff S, Barone L, Hsu HP, Wrenn C, Gagne T, Chi T. Healing of chondral and osteochondral defects in a canine model: the role of cultured chondrocytes in regeneration of articular cartilage. *Biomaterials*. 1996;17:147–154.
10. Amiel D, Coutts RD, Abel M, Stewart W, Harwood F, Akeson WH. Rib perichondrial grafts for the repair of full-thickness articular-cartilage defects. A morphological and biochemical study in rabbits. *J Bone Joint Surg Am*. 1985;67:911–920.
11. Sumen Y, Ochi M, Ikuta Y. Treatment of articular defects with meniscal allografts in a rabbit knee model. *Arthroscopy*. 1995;11:185–193.
12. Hoikka VE, Jaroma HJ, Ritsila VA. Reconstruction of the patellar articulation with periosteal grafts. 4-year follow-up of 13 cases. *Acta Orthop Scand*. 1990;61:36–39.
13. Matsusue Y, Yamamuro T, Hama H. Arthroscopic multiple osteochondral transplantation to the chondral defect in the knee associated with anterior cruciate ligament disruption. *Arthroscopy*. 1993;9:318–321.
14. Zhang F, He Q, Tsang WP, Garvey WT, Chan WY, Wan C. Insulin exerts direct, IGF-1 independent actions in growth plate chondrocytes. *Bone Res*. 2014;2:14012.
15. Shen J, Li S, Chen D. TGF-beta signaling and the development of osteoarthritis. *Bone Res*. 2014;2:14002.
16. Langer R, Vacanti JP. Tissue engineering. *Science*. 1993;260:920–926.
17. Ye K, Felimban R, Moulton SE, et al. Bioengineering of articular cartilage: past, present and future. *Regen Med*. 2013;8:333–349.
18. Vats A, Tolley NS, Polak JM, Buttery LD. Stem cells: sources and applications. *Clin Otolaryngol Allied Sci*. 2002;27:227–232.
19. Turksen K. Revisiting the bulge. *Dev Cell*. 2004;6:454–456.
20. Grottkau BE, Purudappa PP, Lin YF. Multilineage differentiation of dental pulp stem cells from green fluorescent protein transgenic mice. *Int J Oral Sci*. 2010;2:21–27.
21. Levi B, Longaker MT. Concise review: adipose-derived stromal cells for skeletal regenerative medicine. *Stem Cells*. 2011;29:576–582.
22. Mizuno H, Tobita M, Uysal AC. Concise review: adipose-derived stem cells as a novel tool for future regenerative medicine. *Stem Cells*. 2012;30:804–810.
23. Erickson GR, Gimble JM, Franklin DM, Rice HE, Awad H, Guilak F. Chondrogenic potential of adipose tissue-derived stromal cells in vitro and in vivo. *Biochem Biophys Res Commun*. 2002;90:763–769.
24. Pham QP, Sharma U, Mikos AG. Electrospun poly(epsilon-caprolactone) microfiber and multilayer nanofiber/microfiber scaffolds: characterization of scaffolds and measurement of cellular infiltration. *Biomacromolecules*. 2006;7:2796–2805.
25. Tuzlakoglu K, Bolgen N, Salgado AJ, Gomes ME, Piskin E, Reis RL. Nano- and micro-fiber combined scaffolds: a new architecture for bone tissue engineering. *J Mater Sci Mater Med*. 2005;16:1099–1104.
26. Coti KK, Belowich ME, Liong M, et al. Mechanised nanoparticles for drug delivery. *Nanoscale*. 2009;1:16–39.
27. Zhou S, Deng X, Yang H. Biodegradable poly(epsilon-caprolactone)-poly(ethylene glycol) block copolymers: characterization and their use as drug carriers for a controlled delivery system. *Biomaterials*. 2003;24:3563–3570.
28. Xie J, MacEwan MR, Schwartz AG, Xia Y. Electrospun nanofibers for neural tissue engineering. *Nanoscale*. 2010;2:35–44.
29. Bakandritsos A, Mattheolabakis G, Zboril R, et al. Preparation, stability and cytocompatibility of magnetic/PLA-PEG hybrids. *Nanoscale*. 2010;2:564–572.
30. Ishaug SL, Crane GM, Miller MJ. Bone formation by three-dimensional stromal osteoblast culture in biodegradable polymer scaffolds. *J Biomed Mater Res*. 1997;36:17–28.
31. Goldstein AS, Zhu G, Morris GE, Meszlenyi RK, Mikos AG. Effect of osteoblastic culture conditions on the structure of poly(DL-lactic-co-glycolic acid) foam scaffolds. *Tissue Eng*. 1999;5:421–434.
32. Lo H, Kadiyala S, Guggino SE, Leong KW. Poly(L-lactic acid) foams with cell seeding and controlled-release capacity. *J Biomed Mater Res*. 1996;30:475–484.
33. Saad B, Matter S, Ciardelli G, Uhlschmid GK, Welti M, Neuenschwander P. Interactions of osteoblasts and macrophages with biodegradable and highly porous polyesterurethane foam and its degradation products. *J Biomed Mater Res*. 1996;32:355–366.
34. Whang K, Healy KE, Elenz DR, et al. Engineering bone regeneration with bioabsorbable scaffolds with novel microarchitecture. *Tissue Eng*. 1999;5:35–51.
35. Harris LD, Kim BS, Mooney DJ. Open pore biodegradable matrices formed with gas foaming. *J Biomed Mater Res*. 1998;42:396–402.
36. Ji X, Wang T, Guo L, et al. Effection of nano-ZnO on the mechanical property and biocompatibility of electrospun poly(L-lactide) acid/Nano-ZnO mats. *J Biomed Nanotechnol*. 2013;9:417–423.
37. Yang W, Fu J, Wang D, et al. Study on chitosan/polycaprolactone blending vascular scaffolds by electrospinning. *J Biomed Nanotechnol*. 2010;6:254–259.
38. Shi S, Xie J, Zhong J, Lin S, Zhang T, Sun K. Effects of low oxygen tension on gene profile of soluble growth factors in co-cultured

adipose-derived stromal cells and chondrocytes. *Cell Prolif*. 2016;49:341–351.
39. Lin S, Svoboda KK, Feng JQ, Jiang X. The biological function of type I receptors of bone morphogenetic protein in bone. *Bone Res*. 2016;4:16005.
40. Fu N, Deng S, Fu Y, Li G, Cun X. Electrospun P34HB fibres: a scaffold for tissue engineering. *Cell Prolif*. 2014;47:465–475.
41. Fu N, Xie J, Li G. P34HB film promotes cell adhesion, in vitro proliferation, and in vivo cartilage repair. *RSC Adv*. 2015;5:21572–21579.
42. Li G, Fu N, Xie J, et al. Poly(3-hydroxybutyrate-co-4-hydroxybutyrate) based electrospun 3D scaffolds for delivery of autogeneic chondrocytes and adipose-derived stem cells: evaluation of cartilage defects in rabbit. *J Biomed Nanotechnol*. 2015;11:105–116.
43. Chang T, Xie J, Li H, Li D, Liu P, Hu Y. MicroRNA-30a promotes extracellular matrix degradation in articular cartilage via downregulation of Sox9. *Cell Prolif*. 2016;49:207–218.
44. Zhang T, Xie J, Sun K, Fu N, Deng S, Lin S. Physiological oxygen tension modulates soluble growth factor profile after crosstalk between chondrocytes and osteoblasts. *Cell Prolif*. 2016;49:122–133.
45. Zhang X, Guo J, Wu G. Effects of heterodimeric bone morphogenetic protein-2/7 on osteogenesis of human adipose-derived stem cells. *Cell Prolif*. 2015;48:650–660.
46. Zhu Y, Yuan M, Meng HY, et al. Basic science and clinical application of platelet-rich plasma for cartilage defects and osteoarthritis: a review. *Osteoarthritis Cartilage*. 2013;21:1627–1637.
47. Filardo G, Madry H, Jelic M, Roffi A, Cucchiarini M, Kon E. Mesenchymal stem cells for the treatment of cartilage lesions: from preclinical findings to clinical application in orthopaedics. *Knee Surg Sports Traumatol Arthros*. 2013;21:1717–1729.
48. Zhang D, Tong A, Zhou L, Fang F, Guo G. Osteogenic differentiation of human placenta-derived mesenchymal stem cells (PMSCs) on electrospun nanofiber meshes. *Cytotechnology*. 2012;64:701–710.